J. Fluid Mech. (1987), *vol.* 177, *pp.* 49–65
Printed in Great Britain

On the excitation of long nonlinear water waves by a moving pressure distribution. Part 2. Three-dimensional effects

By C. KATSIS AND T. R. AKYLAS
Department of Mechanical Engineering, Massachusetts Institute of Technology, Cambridge, MA 02139, USA

(Received 28 April 1986)

The three-dimensional wave pattern generated by a moving pressure distribution of finite extent acting on the surface of water of depth h is studied. It is shown that, when the pressure distribution travels at a speed near the linear-long-wave speed, the response is governed by a forced nonlinear Kadomtsev–Petviashvili (KP) equation, which describes a balance between linear dispersive, nonlinear and three-dimensional effects. It is deduced that, in a channel of finite width $2w$, three-dimensional effects are negligible if $w \ll h^2/a$, a being a typical wave amplitude; in such a case the governing equation reduces to the forced Korteweg–de Vries equation derived in previous studies. For $aw/h^2 = O(1)$, however, three-dimensional effects are important; numerical calculations based on the KP equation indicate that a series of straight-crested solitons are radiated periodically ahead of the source and a three-dimensional wave pattern forms behind. The predicted dependencies on channel width of soliton amplitude and period of soliton formation compare favourably with the experimental results of Ertekin, Webster & Wehausen (1984). In a channel for which $aw/h^2 \gg 1$, three-dimensional, unsteady disturbances appear ahead of the pressure distribution.

1. Introduction

In the last few years, considerable research activity has focused on the generation of nonlinear waves by moving sources. The original motivation was provided by the experimental observations of Huang *et al.* (1982); they pointed out that ships travelling in channels of finite depth and width at near-critical speeds, i.e. close to the linear-long-wave speed† continuously excite solitons which form and propagate upstream. In spite of the fact that the channel width may be large compared with the dimensions of the ship, these solitons are straight-crested, spanning the entire width of the channel. Similar phenomena have been observed in continuously stratified flow over topography (Baines 1979) and, more recently, in two-layer flow (Baines 1984).

On physical grounds, the importance of nonlinear effects near critical speed, manifested in the appearance of solitons, can be understood as follows: according to linear theory, the generated waves have to be steady in the frame of reference of the moving source, after all initial transients have decayed. As critical speed is

† Soliton radiation was much more intense at near-critical speeds, but small-amplitude upstream disturbances have been observed at Froude numbers as low as 0.2; for high supercritical Froude numbers, wave breaking occurs.

approached, the linear dispersion relation indicates that the steady long waves are almost non-dispersive and that the corresponding group velocity tends to vanish in the moving frame; thus, however small the wave amplitude, nonlinear effects cannot be neglected in comparison with dispersive effects. Furthermore, the vanishing of the group velocity of the generated long waves close to critical conditions implies that the energy transferred by the source to the wave disturbance cannot be easily radiated away, suggesting the possibility that no steady state is reached.

Theoretical evidence for the excitation of solitons near critical conditions was first provided by the numerical calculations of Wu & Wu (1982). Using as excitation a pressure distribution localized in the streamwise direction but entirely uniform in the spanwise direction, they solved numerically the Boussinesq equations and found a series of solitons propagating ahead of the source. In subsequent work, Akylas (1984) (hereinafter referred to as I) demonstrated that, near critical conditions, the linearized water-wave theory is singular in the sense that no linear steady-state response exists; in view of the balance between dispersion and nonlinearity, which occurs close to critical conditions, and the fact that the generated waves follow the source, the appropriate evolution equation is a forced Korteweg–de Vries (KdV). Numerical solutions of the forced KdV again show the appearance of solitons. Extensions of this study have been made by, among others, Cole (1985) and Grimshaw & Smyth (1985) who pointed out, respectively, that the same KdV equation is valid for two-dimensional transcritical flow past a bump and stratified flow over topography. Also, in agreement with the continuous radiation of solitons revealed by the numerical calculations, Miles (1986) recently showed analytically that no nonlinear steady state exists for a certain range of transcritical speeds.

The theoretical work cited above, based on the assumption that the source is uniform in the spanwise direction and, thus, that waves are straight-crested *ab initio* both upstream and downstream, cannot furnish a quantitative description of the experimental findings of Huang *et al.* (1982) and Ertekin *et al.* (1984)†: the experiments indicate that the response is two-dimensional only upstream but three-dimensional downstream; furthermore, soliton-radiation characteristics, such as amplitude and period of formation, depend critically on the so-called blockage coefficient, the ratio of the mid-ship-section area to the cross-section area of the channel.

Three-dimensional aspects of the wave pattern near critical conditions were first explored by Mei (1986) who showed that, for a slender ship advancing in a channel, the response is two-dimensional both upstream and downstream if the channel width $2w$ is not too large: $w \ll h^2/a$, h being the channel depth and a the typical wave amplitude; to leading order, the governing equation is the forced KdV derived in I, the forcing being proportional to the blockage coefficient. The same conclusion was reached by Cole (1986) who, however, restricted the channel width to be comparable to the water depth, $w/h = O(1)$. As far as we are aware, the only theoretical study which can account for the radiation of solitons ahead of the source and the three-dimensional nature of the response behind the source is the recent numerical work of Ertekin, Webster & Wehausen (1986). Following their earlier two-dimensional computations (Ertekin *et al.* 1984), they solved numerically the three-dimensional Green–Naghdi equations in a channel of fixed width, using as a source

† Lee (1985) (see also Wu 1986), however, carried out experiments using a two-dimensional bottom bump moving at transcritical speed as a source and found reasonable quantitative agreement with the predictions of the two-dimensional theory.

a rectangular pressure distribution of width about half the channel width, and examined the variation with speed of the generated straight-crested solitons.

The present work is primarily concerned with the dependence of soliton radiation on channel width. The experiments of Ertekin *et al.* (1984) clearly indicate that the period of soliton formation increases while soliton amplitude decreases as the channel width is increased. This suggests what seems to be intuitively clear: no straight-crested solitons can be radiated upstream for an infinitely wide channel. However, it is conceivable that three-dimensional wave disturbances are radiated, which propagate upstream and slowly disperse in the absence of channel walls.

Our investigation is based on the forced Kadomtsev–Petviashvili (KP) equation. This equation, the three-dimensional counterpart of the forced KdV equation derived in I, is shown to describe the appropriate balance between linear dispersive, nonlinear and three-dimensional effects close to critical speed. Apart from being simpler to handle numerically than the Boussinesq or the Green–Naghdi equations, the KP equation brings out explicitly the weak dependence of the wave pattern on the spanwise direction; in the limit that the channel width is not too large in the sense of Mei (1986), it reduces to the forced KdV equation.

In a finite channel, the linearized KP equation shows that no steady state is reached at critical conditions; as in the corresponding two-dimensional problem, in the absence of nonlinear effects, energy cannot be radiated away from the source. Numerical calculations based on the full KP equation indicate that a series of straight-crested solitons are radiated periodically ahead of the source and a three-dimensional wave pattern forms behind. The predicted dependencies on channel width of soliton amplitude and period of soliton formation compare favourably with the experimental results of Ertekin *et al.* (1984). The extent of validity of the quasi-two-dimensional theory of Mei (1986) is assessed; it is found that the maximum dimensionless channel width aw/h^2 for which the downstream disturbance is more or less two-dimensional depends crucially on the source characteristics. The tendency of solitons to become straight-crested in the presence of sidewalls is further illuminated by solving numerically an initial-value problem with a soliton spanning only half of the channel width as initial condition. It is found that, in agreement with experimental observations of Ertekin (1984), the disturbance very soon adjusts itself so as to form a straight-crested soliton of lower amplitude which spans the entire channel width.

In an unbounded channel, at critical conditions, there exists a linear steady state which, however, involves the displacement of an infinite mass of water from behind to ahead of the source. Numerical calculations, on the other hand, indicate that three-dimensional, unsteady disturbances are generated upstream owing to nonlinear effects, suggesting the possibility that no nonlinear steady state is reached in this case either.

2. Forced KP equation

A prescribed three-dimensional pressure distribution p travelling at constant speed is acting on the free surface of water of uniform depth h, $0 < y < h$. In the frame of reference moving with the source, the pressure is stationary in the presence of a uniform current U in the water. Assuming inviscid and irrotational flow, the ensuing gravity-wave motion is described by the velocity potential $\Phi = Ux - 1/2U^2t + \phi(x, y, z, t)$ and the free-surface elevation $y = h + \eta(x, z, t)$, where x

is the streamwise, y the vertical, and z the spanwise coordinate. We choose dimensionless (primed) variables according to

$$x = lx', \quad y = hy', \quad z = lz', \quad t = \frac{l}{c_0}t', \quad \eta = a\eta', \quad \phi = \frac{agl}{c_0}\phi',$$

$$p = ag\rho p'\left(\frac{l}{L}\xi', \frac{l}{D}\zeta'\right), \quad (1)$$

where l is a typical wavelength, a is a typical wave amplitude, $c_0 = (gh)^{\frac{1}{2}}$ is the linear long-water-wave speed, ρ is the water density, g is the gravitational acceleration, and L, D stand for typical dimensions of the pressure distribution in the streamwise and spanwise directions respectively. In terms of these dimensionless variables, when the primes are dropped, the classical gravity water-wave problem reads

$$\mu^2(\phi_{xx}+\phi_{zz})+\phi_{yy} = 0 \quad (0 < y < 1+\epsilon\eta), \quad (2)$$

$$\eta_t + F\eta_x + \epsilon(\phi_x\eta_x + \phi_z\eta_z) = \phi_y/\mu^2 \quad (y = 1+\epsilon\eta), \quad (3)$$

$$\phi_t + F\phi_x + \eta + \tfrac{1}{2}\epsilon(\phi_x^2+\phi_z^2+\phi_y^2/\mu^2) = -p\left(\frac{x}{\mu}\frac{h}{L}, \frac{z}{\mu}\frac{h}{D}\right) \quad (y = 1+\epsilon\eta), \quad (4)$$

$$\phi_y = 0 \quad (y = 0), \quad (5)$$

where $F = U/c_0$ is the Froude number, $\mu = h/l$ is a measure of dispersion and $\epsilon = a/h$ is a measure of nonlinearity.

According to linear theory ($\epsilon = 0$), the main characteristics of the wave pattern generated by the moving source can be readily deduced from the linear dispersion relation of free gravity water waves:

$$\omega^2 = \frac{k}{\mu}\tanh\mu k, \quad (6)$$

where k is the magnitude of the wavenumber vector and ω is the wave frequency in the stationary reference frame; when the transients induced by the initial acceleration of the source have died out, a wave of wavenumber $\boldsymbol{k}$, inclined at an angle α with respect to the streamwise direction, will persist only if it is stationary in the frame of the moving source (Lighthill 1978 §3.9):

$$\mu^{\frac{1}{2}}Fk\cos\alpha = (k\tanh\mu k)^{\frac{1}{2}}. \quad (7)$$

Equation (7) gives the wavenumber of the wave to be found in the direction α, for any F. Our interest centres on the wave pattern at nearly critical Froude number, $F \approx 1$. Then, condition (7) is satisfied for long waves ($\mu \ll 1$) if $F = 1+O(\mu^2)$ and $\cos\alpha = 1+O(\mu^2)$, implying that the corresponding wave frequency in the frame of the source is $O(\mu^2)$. Therefore, long, almost two-dimensional waves ($k_z/k_x = O(\mu)$) are generated close to critical conditions; for such waves, in the limit $\mu \to 0$, nonlinear effects cannot be neglected in comparison with linear dispersive effects and a balance between dispersion and nonlinearity is anticipated.

To describe quantitatively the wave response close to critical conditions, following the above qualitative arguments, we write

$$F = 1+\lambda\mu^2 \quad (\lambda = O(1)), \quad (8a)$$

and define a stretched spanwise coordinate Z and a slow time T:

$$Z = \mu z, \quad T = \mu^2 t. \quad (8b)$$

Thus, Laplace's equation (2) and the bottom boundary condition (5) give

$$\phi(x,Z,T;y) = f(x,Z,T) - \frac{\mu^2 y^2}{2!} f_{xx} + \frac{\mu^4 y^4}{4!} f_{xxxx} - \frac{\mu^4 y^2}{2!} f_{ZZ} + \ldots; \tag{9}$$

substitution of (9) into the free-surface conditions (3), (4) leads to a set of two coupled equations for f, η

$$\eta_x + f_{xx} + \epsilon(\eta f_{xx} + \eta_x f_x) + \mu^2(\eta_T + f_{ZZ} + \lambda\eta_x - \tfrac{1}{6} f_{xxxx}) = O(\epsilon^2, \mu^4, \epsilon\mu^2), \tag{10a}$$

$$\eta + f_x + \tfrac{1}{2}\epsilon f_x^2 + \mu^2(f_T + \lambda f_x - \tfrac{1}{2} f_{xxx}) = -p + O(\epsilon^2, \mu^4, \epsilon\mu^2). \tag{10b}$$

It is clear now that balance between dispersion and nonlinearity is achieved by the choice $\epsilon = \mu^2$; eliminating f from (10a, b), a single equation for η is obtained to leading order:

$$\eta_{T_x} + \lambda\eta_{xx} - \tfrac{3}{4}(\eta^2)_{xx} - \tfrac{1}{6}\eta_{xxxx} - \tfrac{1}{2}\eta_{ZZ} = \frac{1}{2\epsilon} p_{xx}. \tag{11}$$

This is a forced KP equation, the three-dimensional counterpart of the forced KdV equation derived in I; it brings out the balance between linear dispersive, nonlinear, and thee-dimensional effects which is realized close to critical conditions. The steady version of this equation was previously derived by Mei (1976) for a slender ship moving at transcritical speed, assuming that a steady state exists.

In case the pressure distribution is travelling in a channel of finite dimensionless width $2W$ (as in the experiments of Ertekin *et al.* 1984), the no-flux requirement at the walls $Z = \pm W$ imposes the boundary conditions

$$\eta_Z = 0 \quad (Z = \pm W). \tag{12}$$

The experiments of Ertekin *et al.* (1984) suggest that soliton radiation depends on the blockage coefficient only and not on the precise details of the source; for convenience, we choose the pressure distribution p to be the product of two Gaussians and let $D \sim h$, so that in the limit $\epsilon \ll 1$, we take

$$p\left(\frac{xh}{\epsilon^{\frac{1}{2}}\Lambda}, \frac{Zh}{\epsilon D}\right) = \epsilon p_0 \pi^{\frac{1}{2}} \frac{D}{h} \exp(-\sigma^2 x^2)\, \delta(Z), \tag{13}$$

where $\sigma^2 = h^2/\epsilon L^2$, p_0 is a constant proportional to the total force exerted on the free surface, and δ denotes the Dirac delta function.

Further reduction of the forced KP equation (11) is possible if $W \ll 1$; in this limit, in view of the boundary conditions (12), the free-surface elevation is independent of Z to leading order and, upon integrating (11) with respect to Z across the channel, we find

$$\eta_T + \lambda\eta_x - \tfrac{3}{4}(\eta^2)_x - \tfrac{1}{6}\eta_{xxx} = \frac{\pi^{\frac{1}{2}}}{4} \frac{p_0}{W} \frac{D}{h} \{\exp(-\sigma^2 x^2)\}_x. \tag{14}$$

This is the forced KdV equation derived in I† on which the quasi-two-dimensional theory of Mei (1986) is based. In terms of the dimensional channel width $2w$, the restriction $W \ll 1$ implies that $wa/h^2 \ll 1$ which, as noted by Mei (1986), means that w may be large compared with the water depth and still obtain a two-dimensional response;‡ the extent of validity of this approximation is examined later in §5.2. Also,

† In I, the assumption $L \sim h$ was made so that, in the limit $\epsilon \to 0$, the right-hand side of (14) was found to be proportional to $\delta'(x)$.

‡ Strictly speaking, there is a small, near-field region close to the source where the response is three-dimensional. This region is studied in detail by Cole (1986).

note that the forcing on the right-hand side of (14) of proportional to the parameter $p_0 D/hW$ which is similar to the blockage coefficient defined by Ertekin *et al.* (1984).

3. Linear response

Before embarking on a discussion of the full forced KP equation (11), it is instructive to examine the predictions of the linearized version of (11).

We begin by inquiring whether linear theory predicts a steady-state response at critical conditions ($\lambda = 0$). This question is readily answered for a channel of finite width: integrating the linearized form of (11) across the channel, making use of (13) and the boundary conditions (12), we find

$$\bar{\eta}_T - \tfrac{1}{6}\bar{\eta}_{xxx} = \frac{\pi^{\frac{1}{2}}}{2} p_0 \frac{D}{h} \{\exp(-\sigma^2 x^2)\}_x, \tag{15}$$

where

$$\bar{\eta}(x, T) = \int_{-W}^{W} \eta(x, Z, T)\, \mathrm{d}Z.$$

This is the linearized forced KdV at critical conditions and, as shown in I, the response grows indefinitely with time, $\bar{\eta} \sim T^{\frac{1}{3}}$ as $T \to \infty$. Thus, for W finite, η also grows without bound as $T \to \infty$.

For an unbounded channel ($W \to \infty$), a physically acceptable linear steady state $\eta^{\mathrm{s}}(x, Z)$ exists and can be constructed by standard Green-function techniques:

$$\eta^{\mathrm{s}} = 3^{\frac{3}{4}} 4\pi^{\frac{3}{2}} p_0 \frac{D}{h} \int_0^{\infty} \mathrm{d}\rho \cos \rho^2 Z F(\rho; x), \tag{16}$$

where

$$\begin{aligned} F = {} & \tfrac{1}{2} \exp(-3^{\frac{1}{4}}\rho x) \int_{-\infty}^{x} \mathrm{d}s \exp(-\sigma^2 s^2) \exp(3^{\frac{1}{4}}\rho s) \\ & + \tfrac{1}{2} \exp(3^{\frac{1}{4}}\rho x) \int_{x}^{\infty} \mathrm{d}s \exp(-\sigma^2 s^2) \exp(-3^{\frac{1}{4}}\rho s) \\ & - \int_{-\infty}^{x} \mathrm{d}s \exp(-\sigma^2 s^2) \sin(3^{\frac{1}{4}}\rho(x-s)). \end{aligned} \tag{17}$$

These integrals cannot be evaluated analytically; however, asymptotic approximation is possible far from the source, $|\sigma x| \gg 1$:

$$\begin{aligned} \eta^{\mathrm{s}} \sim {} & 3^{\frac{3}{4}} 4\pi^2 p_0 \frac{D}{h} \frac{1}{\sigma x} \int_0^{\infty} \mathrm{d}\rho \cos \frac{\rho^2 Z}{x^2} \\ & \times \{\tfrac{1}{2} \exp(-3^{\frac{1}{4}}\rho) - \exp(-3^{\frac{1}{2}}\rho^2/4\sigma^2 x^2) \sin 3^{\frac{1}{4}}\rho\} \quad (\sigma x \to +\infty), \end{aligned} \tag{18a}$$

$$\eta^{\mathrm{s}} \sim -3^{\frac{3}{4}} 2\pi^2 p_0 \frac{D}{h} \frac{1}{\sigma x} \int_0^{\infty} \mathrm{d}\rho \cos \frac{\rho^2 Z}{x^2} \exp -3^{\frac{1}{4}}\rho \quad (\sigma x \to -\infty). \tag{18b}$$

Using the method of steepest descents, these expressions can be further simplified along the track of the source ($Z = 0$):

$$\eta^{\mathrm{s}} \sim -3^{\frac{1}{2}} 2\pi^2 p_0 \frac{D}{h} \frac{1}{\sigma x} \quad (Z = 0, |\sigma x| \to \infty). \tag{19}$$

It is worth noting that the finite extent of the pressure distribution cannot be entirely neglected far behind and close to the track of the source ($\sigma x \to \infty$, $Z \to 0$); if, in the

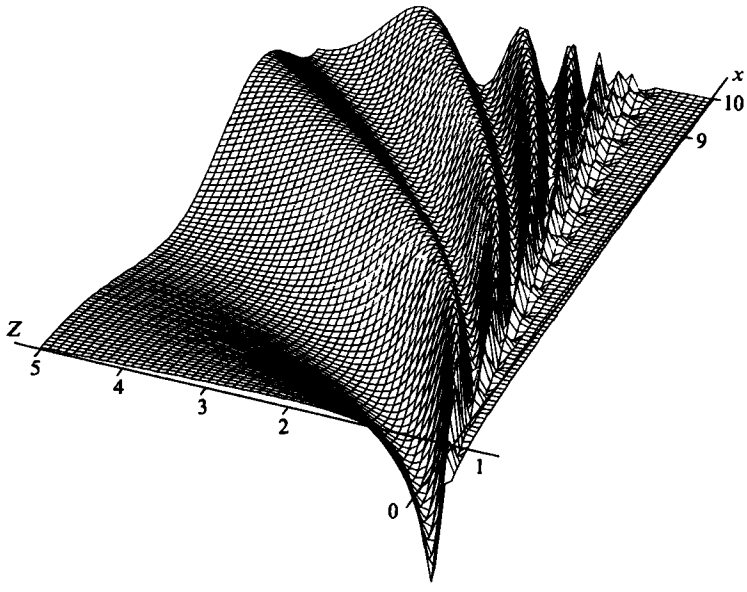

FIGURE 1. Far-field behaviour of the linear steady-state response behind the source (only half of the domain is displayed).

limit $\sigma x \to \infty$, $\exp(-3\frac{1}{2}\rho^2/4\sigma^2 x^2)$ is approximated as 1 in (18*a*), the resulting integral exhibits highly oscillatory behaviour and becomes singular exactly at $Z = 0$. A singularity of the same nature occurs along the track of the classical Kelvin ship-wave pattern (Ursell 1960). Of course, finite-source effects cancel the rapid oscillations close to $Z = 0$ owing to destructive interference.

The details of the steady-state wave pattern far behind the source are shown in figure 1, as computed by numerically evaluating the integrals in (18*a*, *b*). The wave crests have a parabolic shape covering the entire region behind the source. This wave geometry is in close agreement with that predicted by Inui (1936) at critical speed using the full linear-water-wave theory, without making the long-wave assumption inherent in the KP equation. The relatively calm region along the track of the source is the result of destructive interference, as noted earlier. Far ahead of the source, there are no wave crests although there is a finite surface elevation which decays algebraically and contains an infinite amount of mass transferred from behind.

4. Numerical solution of KP

In order to obtain quantitative information about the generated wave pattern, including both dispersive and nonlinear effects, one has to resort to numerical investigation of the forced KP equation (11). It is noteworthy that, although several numerical schemes have been proposed for the KdV in recent years (see Taha & Ablowitz 1984 for a detailed comparison of such schemes), numerical solution of KP does not seem to have been so successful. Only very recently, S. Pierini (1986, unpublished manuscript) presented an implicit, three-level finite-difference scheme for a modified KP equation and studied certain initial-value problems. In this section, an explicit finite-difference method for the standard KP equation is presented.

Assuming that the source is turned on impulsively, the forced KP equation (11) with the forcing (13) is equivalent to the initial-boundary-value problem

$$\eta_{Tx}+\lambda\eta_{xx}-\tfrac{3}{4}(\eta^2)_{xx}-\tfrac{1}{6}\eta_{xxxx}-\tfrac{1}{2}\eta_{ZZ}=0 \quad (-\infty<x<\infty, \quad Z>0, \quad T>0), \tag{20}$$

$$\eta_Z=-p_0\tfrac{1}{2}\pi^{\frac{1}{2}}\frac{D}{h}\{\exp(-\sigma^2x^2)\}_{xx} \quad (-\infty<x<\infty, \quad Z\to 0^+, \quad T>0), \tag{21a}$$

$$\eta=0 \quad (-\infty<x<\infty, \quad Z>0, \quad T=0), \tag{21b}$$

with $$\eta(x,-Z,T)=\eta(x,Z,T) \quad (-\infty<x<\infty, \quad Z\geqslant 0, \quad T\geqslant 0). \tag{22}$$

In discussing the numerical solution, it proves convenient to integrate equation (20) once with respect to x:

$$\eta_T+\lambda\eta_x-\tfrac{3}{4}(\eta^2)_x-\tfrac{1}{6}\eta_{xxx}-\frac{1}{2}\int_{-\infty}^{x}\eta_{ZZ}(s,Z,T)\,\mathrm{d}s=0, \tag{23}$$

where we have made use of the additional information provided by linear-group-velocity arguments, that no waves appear far ahead of the source, so that η and its derivatives vanish there. Working with (23), an explicit numerical scheme of the Lax–Wendroff type, similar to the one used for the KdV in I, is constructed; with the notation

$$\eta^n_{jk}=\eta(j\Delta x, k\Delta Z, n\Delta T),$$

η^{n+1}_{jk} is expanded in a Taylor series:

$$\eta^{n+1}_{jk}=\eta^n_{jk}+\Delta T\eta^n_{Tjk}+\tfrac{1}{2}\Delta T^2\eta^n_{TTjk}+O(\Delta T^3). \tag{24}$$

Making use of (23), η^n_{Tjk} and η^n_{TTjk} are expressed exactly in terms of spatial derivatives and integrals of η; all derivatives are then discretized by centred differences and integrals are evaluated by trapezoidal rule. Also the boundary conditions (12), (21 a) are approximated with second-order, one-sided differences. The resulting scheme is fully explicit and conditionally stable, $\Delta T/\Delta x^3\leqslant 1$, $\Delta T\Delta x/\Delta Z^2\leqslant 1$, with $O(\Delta T^3\Delta x^2)$ local truncation error.

A question that needs to be carefully addressed is that of proper boundary conditions ahead of and behind the source: in a numerical study, the infinite domain $-\infty<x<\infty$ has to be truncated to a finite computational domain $x_{-\infty}\leqslant x\leqslant x_{+\infty}$, say; this necessitates the use of appropriate radiation conditions at $x=x_{\pm\infty}$. As already indicated, ahead of the source at a sufficiently large $x_{-\infty}$, it is consistent to set η and its derivatives equal to zero. Behind the source, however, a radiation boundary condition, which avoids artificial reflections at $x=x_{+\infty}$, is needed. The form of such a boundary condition for the problem at hand, which is nonlinear and involves two spatial dimensions, is unknown. For this reason, we chose to use the rather *ad hoc* boundary condition of setting η and as many x-derivatives as necessary equal to zero at $x=x_{+\infty}$ as well. This condition is admittedly crude but comparison of numerical with exact solutions seems to indicate that, nevertheless, it is useful. Numerical solutions were compared against the exact nonlinear similarity solutions of KP found by Redekopp (1980). Also, as described in the Appendix, it is possible to calculate independently the unsteady linearized response of the forced problem (20), (21) (in an unbounded domain) through Fourier integrals. Comparison of fully numerical solutions with these analytical solutions indicates that, for $T=O(1)$, the effect of the *ad hoc* boundary condition at $x=x_{+\infty}$ is confined close to the boundary and never contaminates more than 15–20 % of the computational domain. Thus, we developed some confidence in our results, obtained after discarding about one fifth

of the computational domain behind the source. See Katsis (1986) for further details concerning the numerical scheme and related error analysis.

5. Nonlinear response in a channel of finite width

In this section, numerical results of the nonlinear evolution of wave disturbances in a channel of finite width are presented. Two types of problems are considered: first, an initial-value problem with a free, straight-crested soliton spanning only half of the channel width as initial condition and, secondly, the forced problem defined by (20), (21) and (12) is discussed.

5.1. *Free-soliton evolution*

Through a linear stability analysis of the KP equation, Kadomtsev & Petviashvili (1970) showed that straight-crested solitons are stable to small-amplitude, three-dimensional perturbations. It is interesting to ask what happens if such perturbations have finite amplitude so that a linear stability analysis is not valid. An experiment which addressed this question in a special setting was carried out by Ertekin (1984 pp. 160–161), who recorded the evolution of an originally straight-crested soliton, travelling in a channel, as it suddenly encounted a section of the channel where the width was larger. He observed that, during a brief transition period, the soliton adjusted its amplitude and speed such that it became straight-crested again and spanned the entire channel width.

This remarkable stability of solitons is investigated here numerically by solving the KP equation (20) in a channel of fixed width, $W = 6.0$, with $\Delta x = 0.125$, $\Delta Z = 0.1$, $\Delta T = 0.001$, using as initial condition a straight-crested soliton of amplitude equal to 1, which spans only half the channel width; this initial-value problem, although it does not mimic precisely the experimental set-up, exhibits similar behaviour and is simpler to handle numerically. One may have misgivings about the discontinuity assumed in the initial condition, in view of the fact that the KP was derived on the assumption of slow three-dimensional variations. However, very similar results are obtained even if the initial discontinuity is smoothed out. The results at three different times are shown in figure 2 (*a–c*). After the initial disturbance is released, it bends backwards and slows down but, as soon as it reflects from the sidewalls, it quickly adjusts to form a straight-crested soliton of lower amplitude; also it appears that this adjustment process, which is reminiscent of soliton diffraction along a convex wall (Miles 1977), is clean in the sense that no appreciable wave disturbance is radiated behind. These conclusions are in qualitative agreement with the experiment of Ertekin (1984) and, as discussed in §6, they play an important part in explaining the radiation of straight-crested solitons by a moving source in the presence of sidewalls. The tendency of a three-dimensional initial disturbance to form two-dimensional solitons was also noted by Pierini (1986) in his numerical calculations using a modified KP.

5.2. *Forced soliton radiation*

The KP equation (20) is solved numerically subject to conditions (12), (21). In the calculations, the choice of parameters

$$\frac{D}{h} = 1, \quad \epsilon = 0.1, \quad \frac{L}{h} = 1, \quad p_0 = \sigma = \epsilon^{-\frac{1}{2}}, \tag{25}$$

is made. Also, $\Delta x = 0.03$, $\Delta Z = 0.02$ and $\Delta T = 0.2 \times 10^{-4}$.

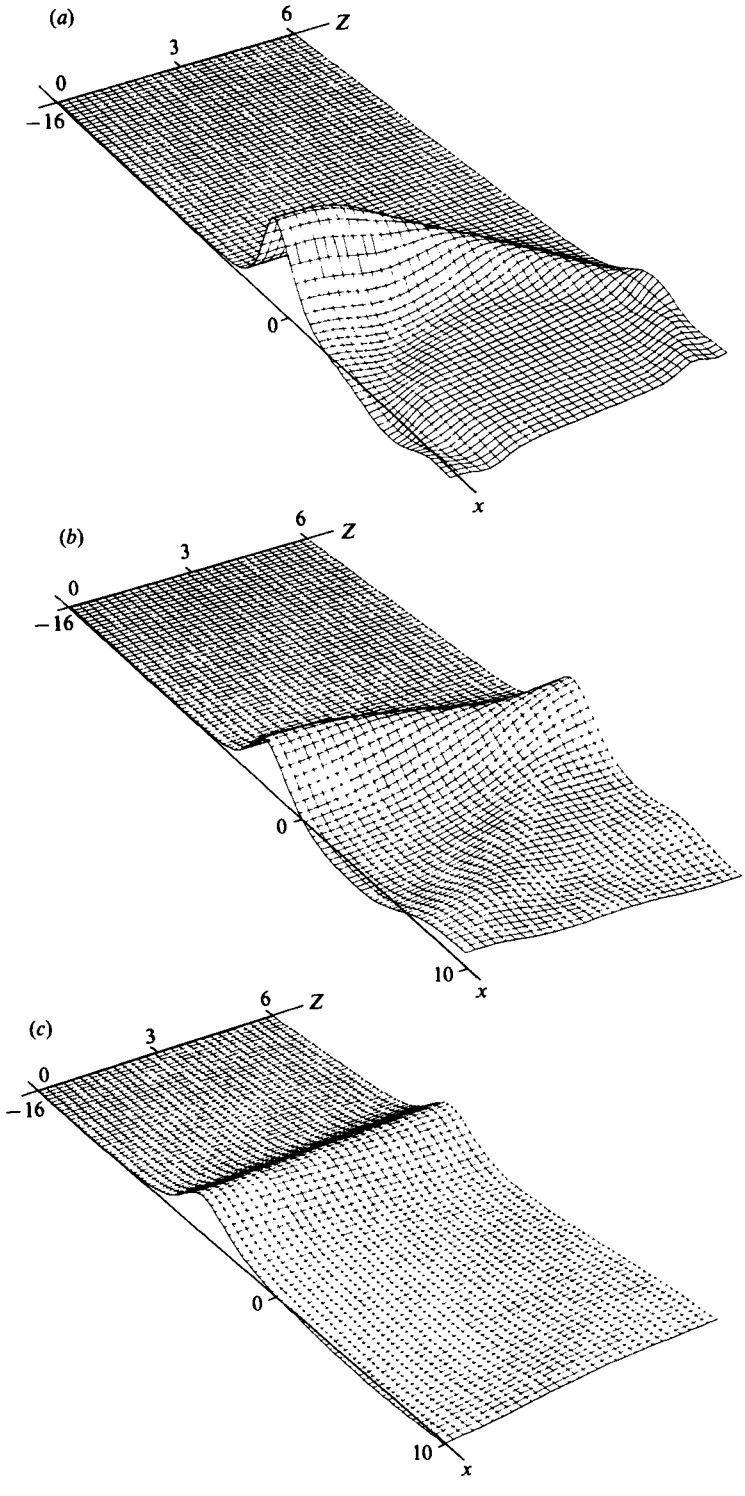

FIGURE 2. Evolution of nonlinear free disturbance from initial condition consisting of a soliton spanning only half of the channel (only half of the domain is displayed); (*a*) $T = 1$, (*b*) $T = 5$, (*c*) $T = 20$.

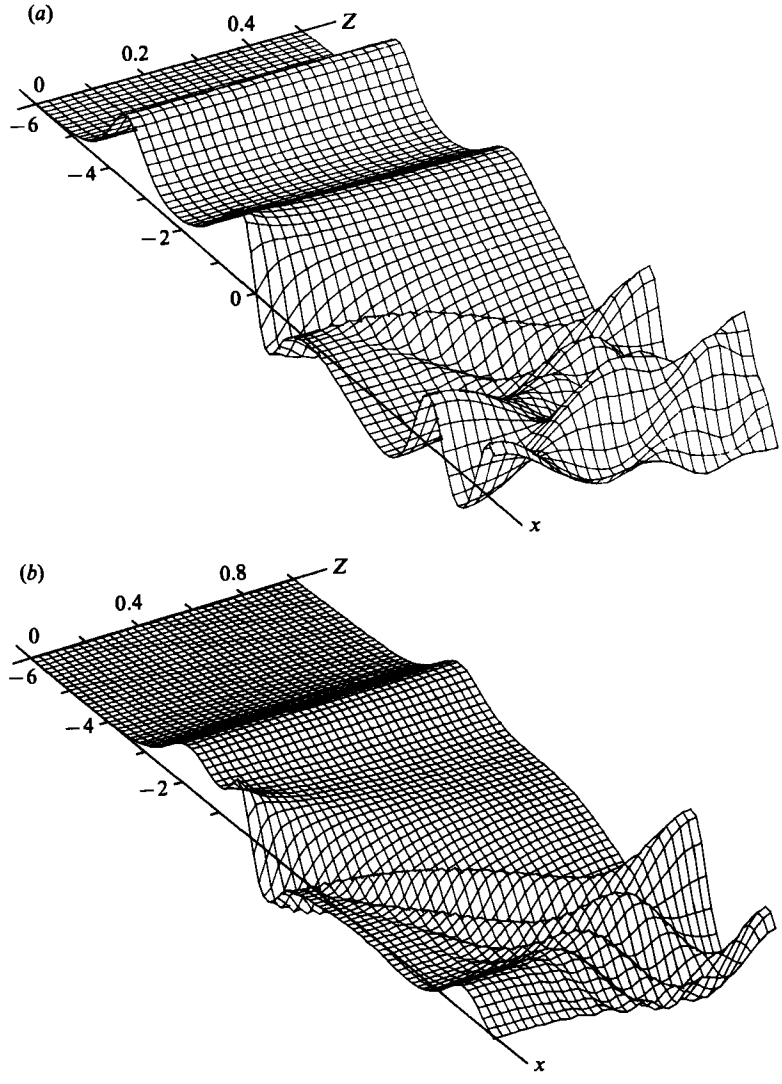

FIGURE 3. Forced nonlinear response at $T = 3$ for $F = 1$ (only half of the domain is displayed); (*a*) Channel width $W = 0.5$, (*b*) $W = 1.0$.

Figure 3(*a*, *b*) shows the response at critical conditions ($\lambda = 0$), at $T = 3.0$, for $W = 0.5$ and $W = 1.0$ respectively. In both cases, straight-crested solitons are radiated ahead of the source; each soliton originally emerges as a three-dimensional disturbance but, as soon as it feels the presence of a sidewall, it adjusts to form a straight-crested soliton and propagates upstream. The period of soliton formation is an increasing function of W while the soliton amplitude is a decreasing function of W. Behind the source, the disturbance is clearly three-dimensional and is quite similar to the one computed by Ertekin *et al.* (1986), with the exception that, in our calculations, the waves downstream are somewhat more pronounced; a similar difference is observed between two-dimensional calculations based on the KdV and the Boussinesq or Green– Naghdi equations (I; Wu & Wu 1982; Ertekin 1984).

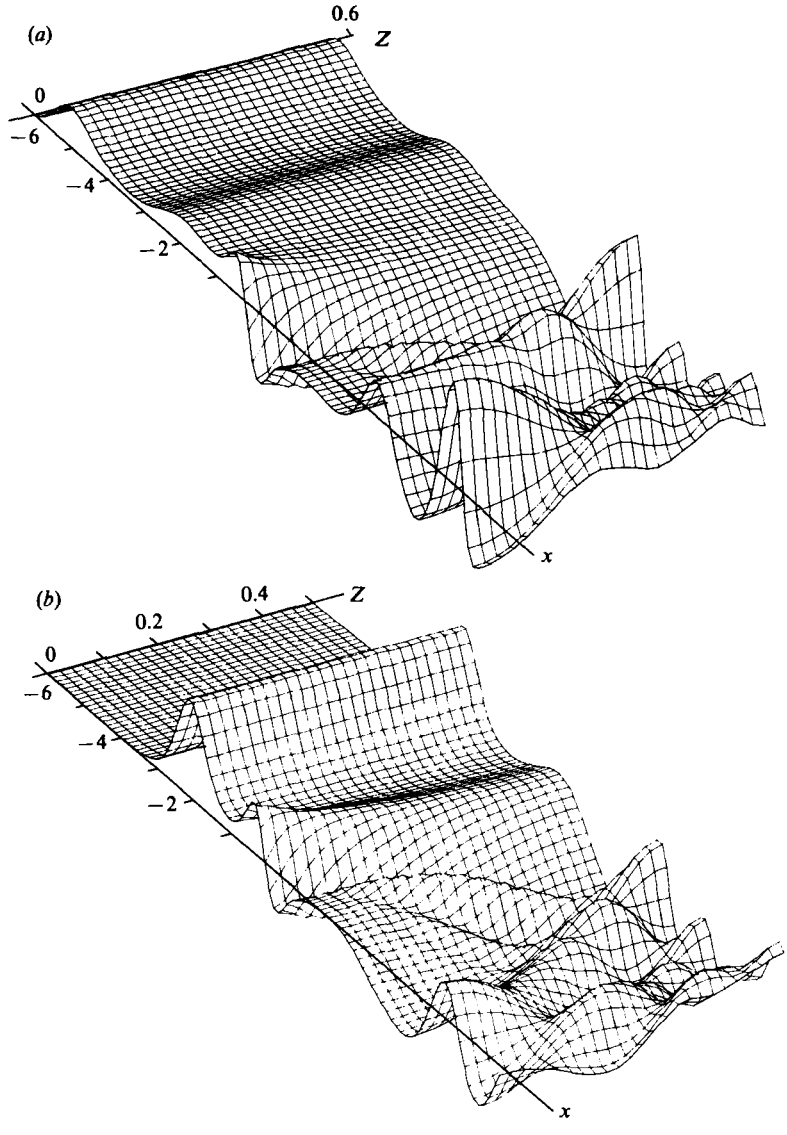

FIGURE 4. Forced nonlinear response at $T = 3$ and channel of fixed width $W = 0.5$ (only half of the domain is displayed); (*a*) $F = 0.9$, (*b*) $F = 1.1$.

The validity of the quasi-two-dimensional approximation of Mei (1986) is examined by investigating the nature of the downstream disturbance as W is decreased. We find that, for the choice of parameters (25), the response behind the source is more or less two-dimensional only if $W \leqslant 0.05$, which places a rather unrealistic restriction on channel width, $w \leqslant 0.5h$. However, for $h/L = \epsilon$, $p_0 = 1$, $\sigma = \epsilon^{\frac{1}{2}}$, which correspond to an elongated source in the streamwise direction, the downstream disturbance is two-dimensional to a reasonable approximation for W as large as 2, $w \leqslant 20h$; in this case, the quasi-two-dimensional theory of Mei (1986) is very useful. Although we have not attempted an exhaustive parametric study, the above results suggest that the maximum W for which the downstream disturbance remains two-dimensional depends crucially on the source characteristics.

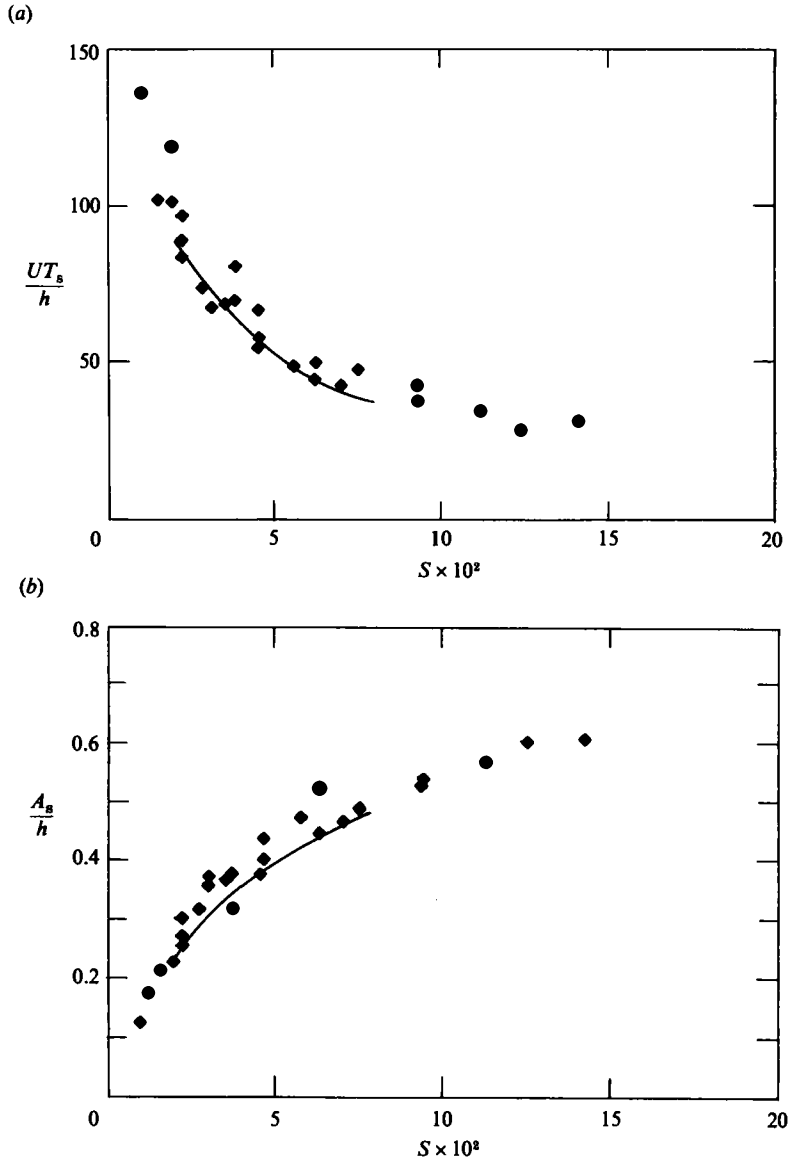

FIGURE 5. Comparison of theoretical estimates of soliton period and amplitude with experiment, for $F = 1$. (*a*) period of soliton formation, T_s, made dimensionless with h/U, as a function of the blockage coefficient S, (*b*) soliton amplitude, A_s, made dimensionless with h, as a function of S; ◆, experimental results of Ertekin, Webster & Wehausen (1984).

The dependence of soliton radiation on source speed is illustrated in figure 4(*a*, *b*) where the response for $W = 0.5$, at $T = 3.0$, and for two Froude numbers, $F = 0.9$ and $F = 1.1$, respectively, are shown. As in the two-dimensional problem, both the period of soliton formation and soliton amplitude increase as the Froude number is increased.

All the trends of the numerical predictions concerning soliton radiation, noted above, are at least in qualitative agreement with experiment. To make a quantitative comparison, we have to be able to relate the ships used in the experiments of Ertekin

et al. (1984) to equivalent pressure distributions; in particular, we need to find the equivalent blockage coefficient of a pressure source. It is not clear how such a calculation could be made from first principles and, for this reason, we adopted the following heuristic approach: the blockage coefficient S is inversely proportional to W,

$$S = \frac{C}{W}, \tag{26}$$

and, in order to determine a value for C, we insist that, for a certain W, the dimensionless amplitude observed by Ertekin *et al.* (1984) agrees with the computed one. Thus, we get $C \approx 2 \times 10^{-2}$. Now, using this value for C, soliton amplitudes (made dimensionless with h) and periods of soliton formation (made dimensionless with h/U), computed for different values of W, are plotted against S. The results are shown in figure 5(a, b) for $F = 1$ together with the experimental points. The agreement is very good for both amplitude and period, confirming the experimental observation that soliton-radiation characteristics depend heavily on the blockage coefficient. It is possible that this surprisingly good agreement is partly due to the fact that, as in the experiments, the theoretical periods and amplitudes were estimated close to the source, perhaps before the radiated solitons had reached steady state; this point is further discussed by Mei (1986).

6. Nonlinear response in an unbounded sea

It was concluded in §5 that the period of soliton formation increases while soliton amplitude decreases as the channel width is increased. This trend clearly suggests (as Ertekin's experiments also did to him) that, in the limit that the channel width becomes infinite ($W \to \infty$), no straight-crested solitons appear; however, generation of three-dimensional, unsteady, upstream disturbances is not precluded and, thus, the question as to whether a nonlinear steady state is reached or some unsteadiness persists still remains. This topic is taken up here.

Using the numerical scheme described in §4 with $\Delta x = 0.05$, $\Delta Z = 0.035$, $\Delta T = 1.2 \times 10^{-4}$ and the same choice of parameters as in (25), the KP equation (20), subject to conditions (21), was solved numerically, taking special care that the response did not reach the boundary of the computational domain in the spanwise direction; this was achieved by constantly increasing the computational domain in the Z-direction. The response at $T = 6$ for $F = 1$ is shown in figure 6. A three-dimensional wave of elevation forms upstream which, as time increases, tends to become less curved and propagates slowly ahead of the source. The fact that this is a purely nonlinear phenomenon is demonstrated in figure 7, where both linear and nonlinear response on the track of the source ($Z = 0$) are plotted for $T = 6$, $F = 1$: the linear disturbance does not show any sign of developing an upstream wave crest; only a slow transfer of water ahead of the source from behind can be detected which eventually leads to the linear steady state discussed in §3.

The appearance of an upstream wave disturbance as $W \to \infty$ suggests that the mechanism of soliton formation in a channel of finite width can be understood as follows: independently of the presence of sidewalls, nonlinear effects lead to the formation of waves of elevation which are curved as they emerge upstream; as soon as they feel the presence of sidewalls, these waves rapidly become straight-crested and propagate upstream, in a way more or less similar to that described in §5.1 for free solitons. This argument also seems to explain the experimentally observed fact

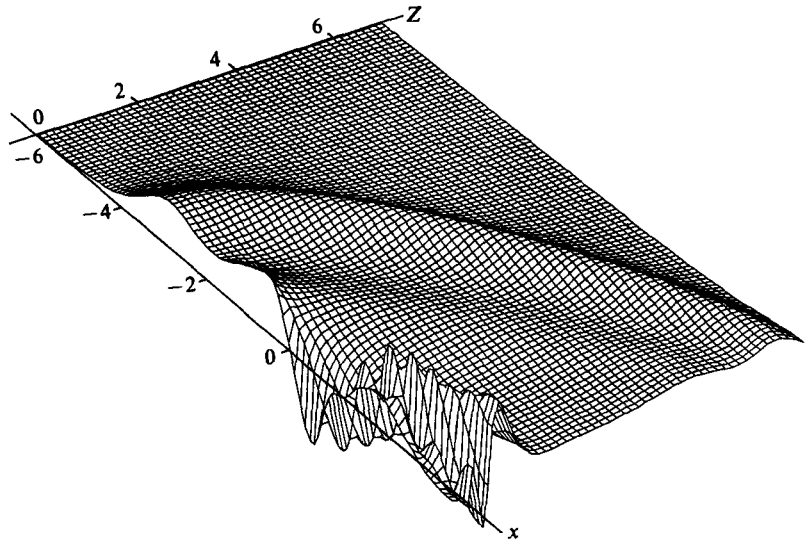

FIGURE 6. Nonlinear forced response in an unbounded channel at $T = 6$ for $F = 1$ (only half of the domain is displayed).

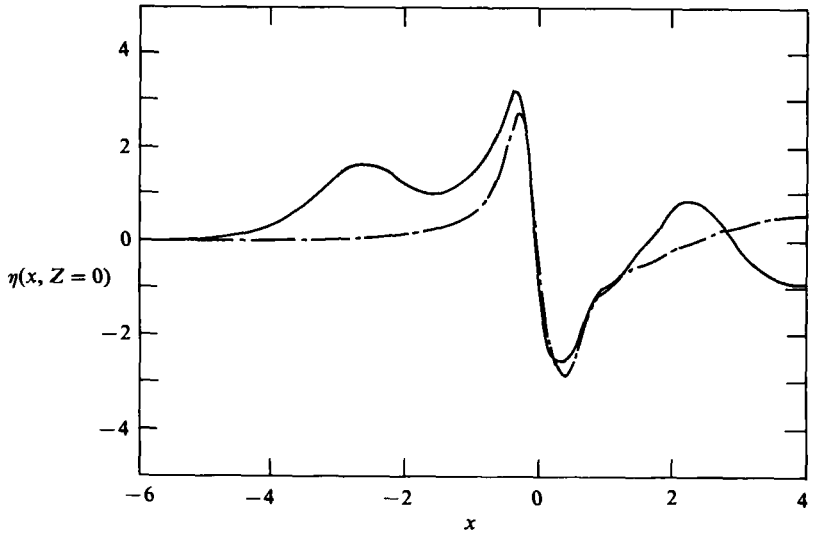

FIGURE 7. Response in an unbounded channel along the track of the source at $T = 6$ for $F = 1$; ——, nonlinear; –·–·–, linear.

that, although soliton amplitude decreases as W increases, soliton mass increases: for $T \leqslant O(1)$, the mass of the upstream disturbance shown in figure 6 increases with time, so that more mass is available for the formation of a straight-crested soliton when the disturbance hits the channel sidewalls; thus, it appears that the presence of sidewalls is not essential for radiating upstream waves but plays an important part in transforming these waves to straight-crested solitons.

A question which has not been answered definitively is whether just one or a series of upstream disturbances are radiated as $W \to \infty$. The answer to this question, which is closely related to the existence of a nonlinear steady state, seems to depend on whether or not the upstream disturbance shown in figure 6 is eventually detached

completely from the main disturbance so that it does not feel the presence of the source. If that is the case, and our numerical calculations suggest that it is, a series of curved waves should be anticipated ahead of the source; otherwise, it is possible that only a single wave appears and its overall mass keeps increasing as it tends to become less curved with time. Owing to the rapid increase of the computational domain, which makes runs prohibitively expensive for large T, we have been unable to carry the computation to times large enough to answer this question in an entirely convincing way. Nevertheless, the tendency to radiate upstream disturbances as $W \to \infty$, revealed by our computations, points to the fact that this is a plausible mechanism for the generation of solitons in the open sea; in the presence of some topography, such disturbances would tend to form straight-crested solitons.

The authors would like to thank Professors C. C. Mei, J. W. Miles, J. V. Wehausen, and T. Y. Wu for valuable discussions on this topic. Also, special thanks are due to Professor A. T. Patera for making available his computer facilities. This work was supported by the Office of Naval Research under project NR062–742. The numerical computations were performed on a Cray-XMP at the Boeing Computer Center under the National Science Foundation Grant MSM-8451154.

Appendix. Linear unsteady response

The linear, unsteady, response in an unbounded sea can be obtained through a fully numerical solution of the linearized version of the KP equation (20), subject to conditions (21). However, in this case, it is also possible to find an analytical solution in terms of Fourier integrals, which can be evaluated without making use of the *ad hoc* radiation condition described in §4. Thus, the two approaches may be compared and the error due to the false boundary condition can be estimated.

Using standard Fourier-integral methods, the linear response in an infinite domain ($W \to \infty$), at critical conditions ($\lambda = 0$), is found to be

$$\eta = \frac{p_0}{\pi^{\frac{1}{2}}\sigma}\frac{D}{h}\left(\frac{2}{T}\right)^{\frac{1}{3}} \mathrm{Re}\left\{\exp\left(\tfrac{3}{4}\mathrm{i}\pi\right)\int_0^1 \mathrm{d}s \int_0^\infty \mathrm{d}k\, Hk^{\frac{3}{2}}\right\}, \tag{A 1}$$

where

$$H = \exp\left[\mathrm{i}\left(k\frac{\zeta^2}{4s^2} + k\xi - \frac{k^3 s^2}{3}\right) - \frac{k^2}{4\sigma^2}\left(\frac{2}{T}\right)^{\frac{2}{3}}\right], \tag{A 2}$$

and

$$\xi = \left(\frac{2}{T}\right)^{\frac{1}{3}} x, \quad \zeta = \left(\frac{2}{T}\right)^{\frac{2}{3}} Z. \tag{A 3}$$

Straightforward numerical evaluation of the double integral in (A 1) is not convenient owing to poor convergence rate. Instead, we write

$$\eta = \frac{p_0}{\pi^{\frac{1}{2}}\sigma}\frac{D}{h}\left(\frac{2}{T}\right)^{\frac{1}{3}} \mathrm{Re}\left\{\exp\left(\tfrac{3}{4}\mathrm{i}\pi\right)\int_0^\infty k^{\frac{3}{2}} \exp\left[\mathrm{i}\left(k\xi - \frac{k^3}{3}\right) - \frac{k^2}{4\sigma^2}\left(\frac{2}{T}\right)^{\frac{2}{3}}\right] g(k,\zeta)\,\mathrm{d}k\right\}, \tag{A 4}$$

Where g satisfies

$$\frac{\partial g}{\partial k} + \left(\frac{3}{2k} - \mathrm{i}k^2\right) g = \frac{3}{2k} \quad (k > 0, \quad \zeta = 0), \tag{A 5}$$

with

$$g \sim 1 + \mathrm{i}\tfrac{2}{5}k^3 \quad (k \to 0, \zeta = 0), \tag{A 6}$$

and

$$\frac{\partial^2 g}{\partial \zeta^2} + \frac{k^4}{3} g = \mathrm{i}\tfrac{1}{2}k \exp\left(-\tfrac{1}{4}\mathrm{i}k\zeta^2\right) \quad (\zeta > 0) \tag{A 7}$$

with

$$\frac{\partial g}{\partial \zeta} = -\frac{1+\mathrm{i}}{2^{\frac{3}{2}}}\pi^{\frac{1}{2}}k^{\frac{1}{2}} \exp\left(\tfrac{1}{3}\mathrm{i}k^3\right) \quad (\zeta = 0). \tag{A 8}$$

Integrating numerically equation (A 5), subject to (A 6), and equation (A 7), subject to (A 8), which are only ordinary differential equations, g is calculated once and for all in the (k, ζ)-plane. For any time T, then, the linear response at (ξ, ζ) is found by evaluating numerically the single integral displayed in (A 4).

REFERENCES

AKYLAS, T. R. 1984 On the excitation of long nonlinear water waves by a moving pressure distribution. *J. Fluid Mech.* **141**, 455–466.

BAINES, P. G. 1979 Observations of stratified flow over two-dimensional obstacles in fluid of finite depth. *Tellus* **31**, 351–371.

BAINES, P. G. 1984 A unified description of two-layer flow over topography. *J. Fluid Mech.* **140**, 127–167.

COLE, S. L. 1985 Transient waves produced by flow past a bump, *Wave Motion* **7**, 579–587.

COLE, S. L. 1986 Transient waves produced by a moving pressure distribution, *Q. Appl. Maths*, (in press).

ERTEKIN, R. C. 1984 Soliton generation by moving disturbances in shallow water: Theory, computation and experiment. Doctoral dissertation, University of California, Berkeley.

ERTEKIN, R. C., WEBSTER, W. C. & WEHAUSEN, J. V. 1984 Ship-generated solitons, *Proc. 15th Symp. Naval Hydrodyn.* pp. 1–15. National Academy of Sciences, Washington, DC.

ERTEKIN, R. C., WEBSTER, W. C. & WEHAUSEN, J. V. 1986 Waves caused by a moving disturbance in a shallow channel of finite width, *J. Fluid Mech.* **169**, 275–292.

GRIMSHAW, R. H. J. & SMYTH, N. 1985 Resonant flow of a stratified fluid over topography. *The University of Melbourne, Dept Maths Res. Rep. no.* 14-1985.

HUANG, D.-B., SIBUL, O. J., WEBSTER, W. C., WEHAUSEN, J. V., WU, D.-M. & WU, T. Y. 1982 Ships moving in the transcritical range. *Proc. Conf. on Behaviour of Ships in Restricted Waters.* (*Varna, Bulgaria*) vol. 2, pp. 26-1–26-10.

INUI, T. 1936 On deformation, wave patterns and resonance phenomenon of water surface due to a moving disturbance, I. *Proc. Phys.-Math. Soc. Japan* **18**, 60–98.

KADOMTSEV, B. B. & PETVIASHVILI, V. I. 1970 On the stability of solitary waves in weakly dispersing media, *Sov. Phys. Dokl.* **15**, 539–541.

KATSIS, C. 1986 An analytical and numerical study of certain three-dimensional nonlinear wave phenomena. Doctoral dissertation, Department of Mechanical Engineering, MIT.

LEE, S.-J. 1985 Generation of long water waves by moving disturbances. Doctoral dissertation, California Institute of Technology.

LIGHTHILL, M. J. 1978 *Waves in Fluids.* Cambridge University Press.

MEI, C. C. 1976 Flow around a thin body moving in shallow water, *J. Fluid Mech.* **77**, 737–751.

MEI, C. C. 1986 Radiation of solitons by slender bodies advancing in a shallow channel. *J. Fluid Mech.* **162**, 53–67.

MILES, J. W. 1977 Diffraction of solitary waves. *Z. angew. Math. Phys.* **28**, 889–902.

MILES, J. W. 1986 Stationary, transcritical channel flow. *J. Fluid Mech.* **162**, 489–499.

REDEKOPP, L. G. 1980 Similarity solutions of some two-space-dimensional nonlinear wave evolution equations, *Stud. Appl. Maths* **63**, 185–207.

TAHA, T. R. & ABLOWITZ, M. J. 1984 Analytical and numerical aspects of certain nonlinear evolution equations III. Numerical, Korteweg–de Vries equation. *J. Comp. Phys.* **55**, 231–253.

URSELL, F. 1960 On Kelvin's ship-wave pattern. *J. Fluid Mech.* **8**, 418–431.

WU, D.-M. & WU, T. Y. 1982 Three-dimensional nonlinear long waves due to moving surface pressure. *Proc. 14th Symp. Naval Hydrodyn.* pp. 103–129. National Academy of Sciences, Washington, DC.

WU, T. Y. 1986 Periodic generation of solitons by steady moving bodies. *Proc. First International Workshop on Water Waves and Floating Bodies.* Cambridge, MA.